ADVANCES IN ATMOSPHERIC SCIENCES, VOL. 32, DECEMBER 2015, 1617–1627

Effect of Methane Emission Increases in East Asia on Atmospheric Circulation and Ozone

SHANG Lin[1], LIU Yi*[2], TIAN Wenshou[3], and ZHANG Yuli[2]

[1]*Shandong Province Climate Centre, Jinan* 250031

[2]*Key Laboratory of the Middle Atmosphere and Global Environmental Observation, Institute of Atmospheric Physics, Chinese Academy of Sciences, Beijing* 100029

[3]*Key Laboratory for Semi-Arid Climate Change of the Ministry of Education, College of Atmospheric Sciences, Lanzhou University, Lanzhou* 730000

(Received 22 January 2015; revised 10 May 2015; accepted 4 June 2015)

ABSTRACT

We used a fully coupled chemistry–climate model (version 3 of the Whole Atmosphere Community Climate Model, WACCM3) to investigate the effect of methane (CH_4) emission increases, especially in East Asia and North America, on atmospheric temperature, circulation and ozone (O_3). We show that CH_4 emission increases strengthen westerly winds in the Northern Hemisphere midlatitudes, accelerate the Brewer–Dobson (BD) circulation, and cause an increase in the mass flux across the tropopause. However, the BD circulation in the tropics between 10°S and 10°N at 100 hPa weakens as CH_4 emissions increase in East Asia and strengthens when CH_4 emissions increase in North America. When CH_4 emissions are increased by 50% in East Asia and 15% globally, the stratospheric temperature cools by up to 0.15 K, and the stratospheric O_3 increases by 45 ppbv and 60 ppbv, respectively. A 50% increase of CH_4 emissions in North America (with an amplitude of stratospheric O_3 increases by 60 ppbv) has a greater influence on the stratospheric O_3 than the same CH_4 emissions increase in East Asia. CH_4 emission increases in East Asia and North America reduce the concentration of tropospheric hydroxyl radicals (4% and 2%, respectively) and increase the concentration of mid-tropospheric O_3 (5% and 4%, respectively) in the Northern Hemisphere midlatitudes. When CH_4 emissions increase in East Asia, the increase in the tropospheric O_3 concentration is largest in August. When CH_4 emissions increase in North America, the increase in the O_3 concentration is largest in July in the mid-troposphere, and in April in the upper troposphere.

Key words: CH_4, temperature, Brewer–Dobson circulation, O_3

Citation: Shang, L., Y. Liu, W. S. Tian, and Y. L. Zhang, 2015: Effect of methane emission increases in East Asia on atmospheric circulation and ozone. *Adv. Atmos. Sci.*, **32**(12), 1617–1627, doi: 10.1007/s00376-015-5028-4.

1. Introduction

Methane (CH_4) is both an important greenhouse and chemically active gas. In the last glacial period (about 18 000 years ago), the concentration of CH_4 was 0.35 ppmv, but it reached 0.75 ppmv in the mid-19th century (e.g., Rasmussen and Khalil, 1984; Chappellaz et al., 1990). With the growth of human activities, the tropospheric CH_4 concentration reached 1.72 ppmv in 1995 (e.g., Lelieveld et al., 1998). Zhang et al. (2001) showed that from the end of the 20th century to the beginning of the 21st century, CH_4 emissions increased by 45% during three decades. Ramaswamy et al. (2001) pointed out that when the 1750 CH_4 mixing ratio of 0.72 ppmv increased to 1.77 ppmv in 2005, a radiative forcing of 0.48 ± 0.05 W m^{-2} was the result. CH_4 is the second most influential radiative-forcing greenhouse gas after CO_2, excluding water vapor.

After the signing of the Montreal Protocol, atmospheric ozone (O_3) depleting substances (ODSs) such as chlorides have been slowly reduced, while CH_4 may continue to increase significantly during the next 50 years. Satellite data show that in East Asia, with China's rapid economic growth, the concentration of pollutants has continued to grow in recent years. Bergamaschi et al. (2013) found that from 2003 to 2008 CH_4 emissions caused by human activities grew fastest in China (18.6 Tg yr^{-1}) — far faster than Brazil with the second fastest growth rate of 2.5 Tg yr^{-1}. Zhang et al. (2011) analyzed Atmospheric Infrared Sounder satellite data and found that, compared with several major countries worldwide, the growth rate of CH_4 emissions has been significantly higher in China than other countries since 2007.

In addition to changing the energy balance of the Earth's atmosphere through the greenhouse effect, CH_4 emission increases also affect water vapor and the O_3 concentration in the stratosphere. Most CH_4 is oxidized in the troposphere

* Corresponding author: LIU Yi
Email: liuyi@mail.iap.ac.cn

by hydroxyl radicals (OH) (e.g., Levy, 1971), but about 7%–11% of CH_4 is transported into the stratosphere and oxidized (e.g., Born et al., 1990). CH_4 oxidation is an important source of stratospheric water vapor (e.g., Lelieveld and Crutzen, 1992; Fuglestvedt et al., 1996; Shindell et al., 2005). CH_4 emissions increase the O_3 concentration in the troposphere and stratosphere (e.g., Owens et al., 1982, 1985; Isaksen and Stordal, 1986; Wuebbles and Hayhoe, 2002). During the 20th century, the global background O_3 concentration rose by at least a factor of two, due mainly to increases in CH_4 and nitrogen oxides (NO_x) emissions (e.g., Marenco et al., 1994; Wang and Jacob, 1998).

Based on a series of model simulations, Butchart and Scaife (2001) found that mass flux transported from the tropical troposphere to stratosphere increases at a rate of 3% (10 yr)$^{-1}$ under conditions of increasing greenhouse gases, as supported by the Intergovernmental Panel on Climate Change (IPCC) emissions scenarios. Increasing greenhouse gases enhances wave activities in the lower stratosphere and accelerates the Brewer–Dobson (BD) circulation (e.g., Rind et al., 2001; Sigmond et al., 2004; Butchart et al., 2006). O_3, water vapor and other trace gases in the troposphere are transported into the stratosphere faster as the BD circulation strengthens (e.g., Austin et al., 2007). Austin and Li (2006) found that greenhouse gas and BD circulation increases jointly lead to increased CH_4 transport into the stratosphere, which is then oxidized into water vapor. The increase of stratospheric water vapor reduces the average age of the atmosphere in the stratosphere. The average age of the atmosphere indicates the transport time scales of substances leaving the troposphere and entering into the stratosphere (e.g., Hall and Plumb, 1994; Waugh and Hall, 2002).

The effects of a CH_4 concentration increase on atmospheric radiation and chemistry has been studied extensively (e.g., Shindell et al., 2005; Chen et al., 2006; Shi, 2006; Bi et al., 2007, 2008; Guo et al., 2008; Bi, 2009; Shi et al., 2009; Xie et al., 2013). Gruzdev and Brasseur (2005) used a two-dimensional model SOCRATES (Simulation of Chemistry, Radiation, and Transport of Environmentally Important Species, SOCRATES) and found that the stratosphere and middle atmosphere became cooler with an amplitude of less than 1 K when CH_4 was increased by 26%. Dyominov and Zadorozhny (2005) found CH_4 increases can cause an increase in stratospheric O_3 and lead to a warming in the stratosphere. However, the chemistry–radiation–dynamic interactions associated with CH_4 increases have not been well resolved in previous modeling studies, due to the limitation of model performance in the stratosphere. On the other hand, most previous studies have investigated the effects of global-scale CH_4 emission increases on climate and stratospheric O_3, but the effect of a CH_4 emissions increase in East Asia on global temperature and O_3 is also still a popular and controversial issue. Wild and Palmer (2008) used a global chemistry transport model to demonstrate that the spatial extent of O_3 production and loss in the troposphere changes very little despite large projected increases in precursor emissions. Stevenson et al. (2006) used 26 atmospheric chemistry models to reveal that ensemble-mean changes in the tropospheric O_3 burden between 2000 and 2030 range significantly, but the effect of CH_4 increases on the tropospheric O_3 was not addressed. In this paper, we use a fully coupled chemistry–climate model to investigate the impact of a CH_4 emissions increase in East Asia on the stratospheric temperature, circulation and O_3, and tropospheric O_3. The results are compared with the impact of global CH_4 increases and a CH_4 emissions increase in North America, to assess the contribution of anthropogenic emissions in East Asia to climate change.

2. Model description and numerical experiments

We used version 3 of the Whole Atmosphere Community Climate Model (WACCM3), which is a global chemistry–climate model with 66 vertical levels extending from the surface to 4.5×10^{-6} hPa ($\sim$160 km). WACCM3 is based on the software framework of the National Center for Atmospheric Research's Community Atmosphere Model, version 3 (CAM3), and includes all of the physical parameterizations of that model. The governing equations, physical parameterizations and numerical algorithms used in CAM3 are documented by Collins et al. (2004), and only the gravity wave drag and vertical diffusion parameterizations are modified in WACCM3. The WACCM3 chemistry module is derived from the three-dimensional chemical transport model MOZART (Model for Ozone and Related Chemical Tracers) (e.g., Brasseur et al., 1998; Hauglustaine et al., 1998; Horowitz et al., 2003). This model resolves 51 neutral species, including all members of the O_x (oxides), NO_x, HO_x (hydrogen oxides), ClO_x (chlorine oxides) and BrO_x (bromine oxides) chemical families, along with tropospheric "source species" such as N_2O (nitrous oxide), H_2O, CH_4, chlorofluorocarbons (CFCs) and other halogenated compounds. WACCM3 performs well in simulating chemical and other atmospheric processes (e.g., Garcia et al., 2007; Eyring et al., 2010; Liu and Liu, 2009). Compared with observation, its simulations tend to be too warm in the Arctic winter, and produce cold temperatures and westerly winds that persist for too long in the Antarctic spring (e.g., Garcia et al., 2007). These biases influence the temperature and O_3 concentration in the polar regions, so the simulation results in the polar regions are not discussed in detail in this study.

We conducted six simulations at a horizontal resolution of $4^\circ \times 5^\circ$ with interactive chemistry, including one control experiment and five sensitivity experiments, listed in Table 1. The surface emissions of CO_2, CH_4, Cl (chlorine), Br (bromine) and 14 other ODSs used in the control run (E0) are 12-month climatologies derived from IPCC's A1B scenario (IPCC, 2007) averaged over the period from 1979 to 2006. The A1 scenario means a future world of very rapid economic growth, a global population that peaks mid-century and declines thereafter, and the rapid introduction of new and more efficient technologies. Under the A1B scenario, technological changes occur in the energy system in a balanced manner across all sources. It has also been widely used in previous

Table 1. Summary of experiments.

Experiment	Location	Averaged CH_4 concentration
E0	East Asia	1.73 ppmv
E15	East Asia	Increase by 15% compared with E0
E30	East Asia	Increase by 30% compared with E0
E50	East Asia	Increase by 50% compared with E0
A50	North American	Increase by 50% compared with E0
G15	Global	Increase by 15% compared with E0

chemistry–climate model simulations in the literature to represent past and future ODS variations. The SST and sea ice fields used in the model are 12-month climatologies derived from Rayner et al. (2003). According to the IPCC 2007 A1B scenario, globally averaged CH_4 emissions increased by 15% in 2006, compared to 1979, and are expected to increase by 50% in 2050, meaning CH_4 emissions will increase observably in the future. In order to study the effect of different CH_4 emission increases in East Asia, in experiments E15, E30 and E50 we forced the surface CH_4 emissions in East Asia to increase by 15%, 30% and 50%, respectively, compared to experiment E0 (the increments were 7.5, 15 and 25 Tg yr^{-1}, approximately). East Asia was taken to range over the area (0°–90°N, 60°–120°E). In order to study the effect of CH_4 emission increases in different areas, in experiment A50 the surface CH_4 emissions in North America were increased by 50%, the increment (25 Tg yr^{-1}, approximately) and area of which were equal to E50 and the range of North America was taken as (0°–90°N, 60°–120°W). In experiment G15 we forced global surface CH_4 emissions to increase by 15% (increment: 90 Tg yr^{-1}, approximately). The simulations were run for 50 years (from 2000 to 2050), with the first 10 years used as model spin-up, and the remaining 40 years (from 2010 to 2050) of model outputs used for analysis.

3. Effect of CH_4 emission increases on stratospheric temperature and circulation

Figure 1 shows the stratospheric temperature differences of E15, E30, E50, A50 and G15 relative to that in E0. When CH_4 emissions increase by 15% in East Asia, the temperature increases in the lower stratosphere in the Southern Hemisphere, but the temperature differences are not statistically significant (Fig. 1a). When CH_4 emissions increase by 30% in East Asia, there is a weaker temperature decrement in the lower stratosphere of the Southern Hemisphere compared with E15, but the temperature increases in the upper stratosphere (Fig. 1b). The temperature difference is still not sta-

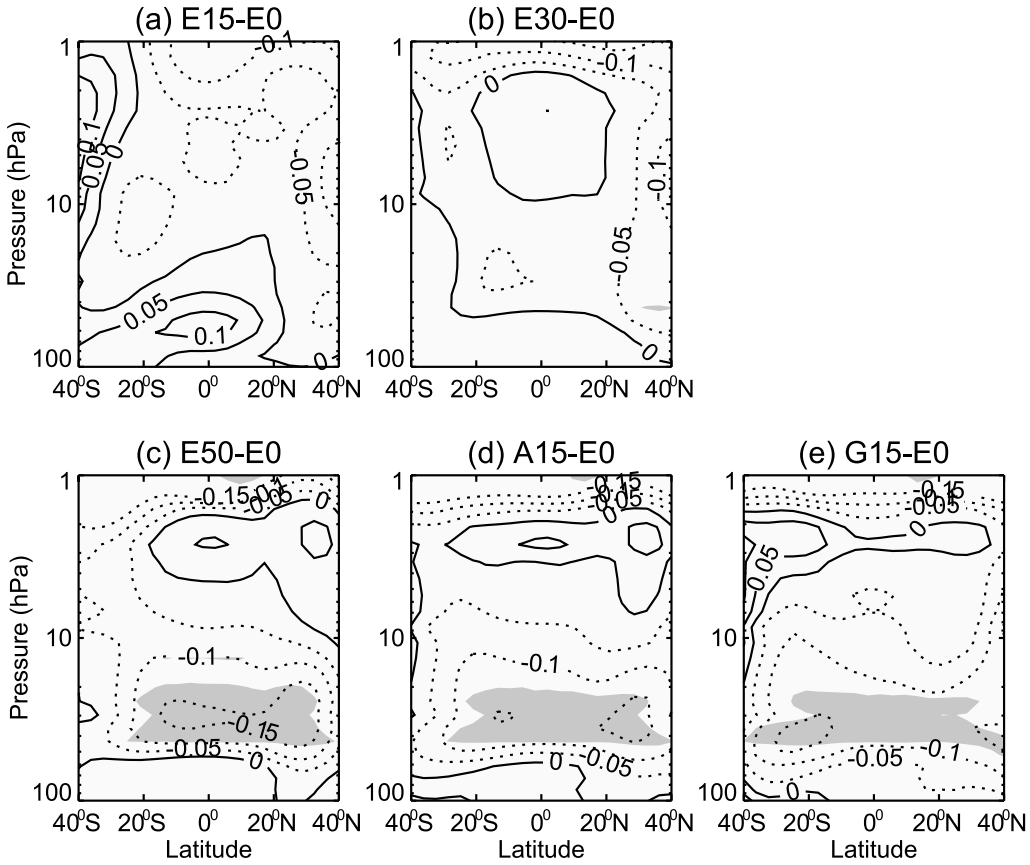

Fig. 1. Latitude–height cross sections of temperature differences (units: K) in (a) E15, (b) E30, (c) E50, (d) A50 and (e) G15, relative to E0. Shaded regions show where the differences are statistically significant at the 90% confidence level, using the Student's *t*-test.

tistically significant in E30 either. When compared with the temperature differences induced by CH_4 emission increases of 15% and 30%, a significant climate effect appears when CH_4 increases in East Asia by 50%, causing the middle stratosphere to cool significantly with a maximum cooling of 0.15 K at 30°N at 50 hPa (Fig. 1c). Therefore, we base our conclusions on the results of E50 when studying the climate effect of CH_4 emission increases in East Asia in the following analysis. Figure 1 also indicates that a 50% CH_4 increase in North America causes a cooling in the middle stratosphere, with a maximum of 0.15 K at 30°N at 50 hPa. When global CH_4 emissions increase by 15%, the amplitude of the stratosphere maximum cooling is similar to that in E50 at 20°S at 60 hPa, but the range of cooling is larger than that in E50. That is to say, the greenhouse effect is much larger in experiment G15 than E50.

Figure 2 shows the differences of the Eliassen–Palm (EP) flux and BD circulation of experiments E50, A50 and G15 compared with experiment E0. The BD circulation is a global-scale cell in the stratosphere in which air rises in the tropics and then moves polewards and downwards, mostly in the winter hemisphere. The BD circulation describes Lagrangian-mean transport and the transformed Eulerian mean residual velocities ($\boldsymbol{v}^*$, $\boldsymbol{w}^*$) (e.g., Andrews and McIntyre, 1976, 1978), which approximate the mean meridional mass transport for seasonally averaged conditions (e.g., Holton, 1990). When CH_4 emissions increase, the stratospheric westerly weakens in the Southern Hemisphere midlatitudes and the mid-stratospheric westerly in the Northern Hemisphere strengthens. Compared with E0, the maximum westerly increment appears in the Northern Hemisphere in E50 and A50, and in the Southern Hemisphere in G15: the location is consistent with Fig. 1, where the temperature gradient is evident. When the extratropical temperature gradient increases, the westerly and wave activity increase (e.g., Eichelberger and Hartmann, 2005; Olsen et al., 2007; Garcia and Randel, 2008). As shown in Fig. 2, as the wave force becomes stronger in the Northern Hemisphere midlatitudes, the vertical velocity of BD circulation speeds up. So, the changes of the mean zonal wind, EP flux and BD circulation are consistent, as shown in Fig. 2. Fomichev et al. (2007) found that the EP flux increases when the westerly is stronger at midlatitudes and the wave flux change in the range 20°–40°N is responsible for the tropical upwelling change. Garcia and Randel (2008) found that the maximum increase of EP flux appeared in the tropics during 1950–2003, and in the midlatitudes during 1980–2050, causing the BD circulation to change accordingly. It is worth noting that the vertical velocity of EP flux at 100 hPa in the Northern Hemisphere midlatitudes changes most significantly in all the sensitivity experiments, and the vertical velocity of BD circulation also increases significantly south of the equator in A50; but, in E50 and G15, the vertical velocity of BD circulation reduces south of the equator at 100 hPa. This is further analyzed later

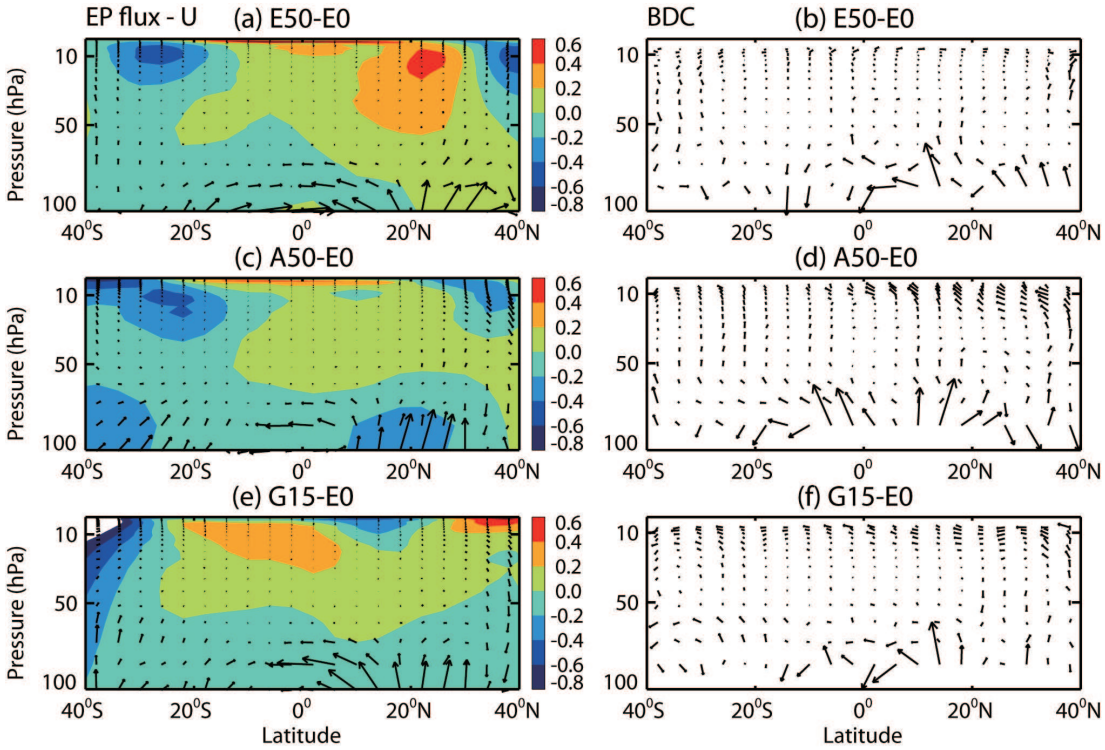

Fig. 2. Latitude–height cross sections of (a, c, e) EP flux (arrows), where shading represents the differences of the average zonal westerly winds (units: m s^{-1}), with positive change indicating strengthening westerlies and negative change indicating weakening westerlies; and (b, d, f) BD circulation differences (arrows): (a, b) E50 relative to E0; (c, d) A50 relative to E0; (e, f) G15 relative to E0.

in the paper.

Using a series of models (including WACCM), Butchart et al. (2006) found that BD circulation upwelling regions extend roughly 30° either side of the equator, though there are variations in the width of about 10° between the models. In our simulations, the BD circulation rises between 22°S and 30°N under the SST and greenhouse gas concentrations used. So, the region between 22°S and 30°N is defined as the BD circulation rising zone. Lin and Fu (2013) found that the acceleration rate of the BD circulation is much larger in the lower stratosphere than upper stratosphere as greenhouse gas concentrations increase. As previous studies have used the upward mass flux across 100 hPa to infer the strength of the BD circulation (e.g., Garcia and Randel, 2008; Garny et al., 2011), Table 2 shows the changes of upward mass flux of E50, A50 and G15 at different altitudes. The increment of upward mass flux is larger at 100 hPa than at 70 hPa and 30 hPa, i.e., when CH_4 emissions increase (in East Asia, North America and on the global scale) the increment of upward mass flux and the acceleration of the BD circulation is larger in the lower than in the upper stratosphere. It is worth noting that the change of upward mass flux is largest in experiment A50; so, compared with a 50% CH_4 emissions increase in East Asia, there is a larger effect of the CH_4 emissions increase in North America on the EP flux, BD circulation and mass flux.

In order to study the BD circulation vertical velocity difference as CH_4 emissions increase by different concentrations and in different areas, Fig. 3 further shows the difference of the BD circulation vertical velocity between sensitivity experiments and the control experiment E0. When CH_4 emissions increase in East Asia and globally, the difference of $\boldsymbol{w}^*$ is rather small between 22°S and 10°S, while in the equatorial region (10°S–10°N) $\boldsymbol{w}^*$ reduces and $\boldsymbol{w}^*$ is stronger between 10°N and 30°N at 100 hPa. When CH_4 emissions increase in North America, the difference of $\boldsymbol{w}^*$ between 22°S and 10°S is similar to that in other experiments, but it is very different between 10°S–30°N, as in the equatorial region (10°S–10°N) $\boldsymbol{w}^*$ becomes stronger and between 20°–30°N $\boldsymbol{w}^*$ is weaker. In the following analysis, the region between 22°S and 30°N is divided into three parts: 10°–30°N, 10°S–10°N and 10°–22°S.

CH_4 emission increases accelerate the BD circulation, which can transport more air mass from the troposphere into the stratosphere. Table 3 shows the differences of upward mass flux at 100 hPa in experiments E15, E30, E50, A50 and G15, relative to that in experiment E0. Note that the upward mass flux between 10°S and 10°N decreases in all experiments except A50, i.e., E15, E30, E50 and G15, compared to that in experiment E0. The changes of upward mass flux are consistent with BD circulation vertical velocity variations.

Figure 4 shows the seasonal variations of the BD circulation vertical velocity. It is apparent that the vertical velocity variations caused by different levels of increase in CH_4 surface emissions are quite different, although the vertical velocity reduces in January and February in all the sensitivity experiments between 10°S and 10°N, and in this range the BD circulation ascending branch becomes stronger during March and June in E15. This change is not obvious in E30, and the vertical velocity reduces during May and August in E50. Table 3 shows that between 22°S and 10°S the upward mass flux decreases in E15 and E30, but increases in E50. When CH_4 emissions increase in East Asia the increment of upward mass flux between 10°N and 30°N is largest in E30. Above all, the change of upward mass flux at 100 hPa is nonlinear as the CH_4 emissions gradually increase in East Asia in E15, E30 and E50. In A50 the vertical velocity decreases slightly in January and February between 10°S and 10°N and increases obviously between 10°N and 20°N from January to May. The combined effect is that the upward mass flux increment at 100 hPa is largest in A50. There is no obvious change of mass flux between 10°S and 10°N in G15, but the mass flux increase is remarkable between 10°N and 30°N, as

Table 2. The difference of mass flux between E50, A50, G15 and E0 at 100 hPa, 70 hPa and 30 hPa between 22°S and 30°N. Positive values indicate a mass flux increase.

	Mass flux difference (10^6 kg s^{-1})		
Pressure	E50–E0	A50–E0	G15–E0
100 hPa	23.7	141	133
70 hPa	19.1	58.5	51.2
30 hPa	17.2	25.6	11.3

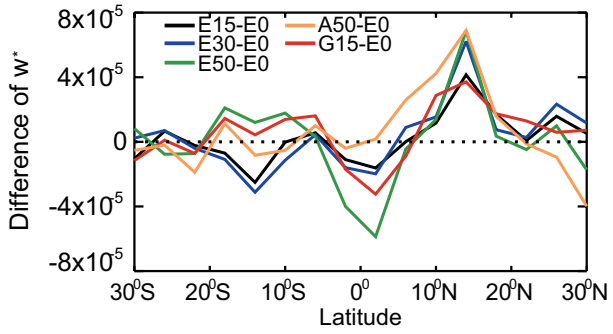

Fig. 3. Difference of BD circulation vertical velocity $\boldsymbol{w}^*$ (units: −Pa s^{-1}) at 100 hPa. Lines represent the difference of E15 (black), E30 (blue), E50 (green), A50 (orange) and G15 (red) relative to E0.

Table 3. The difference of mass flux between each sensitivity experiment and E0 at 100 hPa. Positive values indicate a mass flux increase and negative values indicate a mass flux decrease.

	Mass flux difference (10^6 kg s^{-1})			
Experiment	22°–10°S	10°S–10°N	10°–30°N	22°S–30°N
E0	161	722	258	1060
E15–E0	−50.3	−15.7	115	49.4
E30–E0	−67.5	−28.3	154	57.9
E50–E0	37.8	−105	90.5	23.7
A50–E0	−22.6	106	57.4	141
G15–E0	17.2	−0.39	116	133

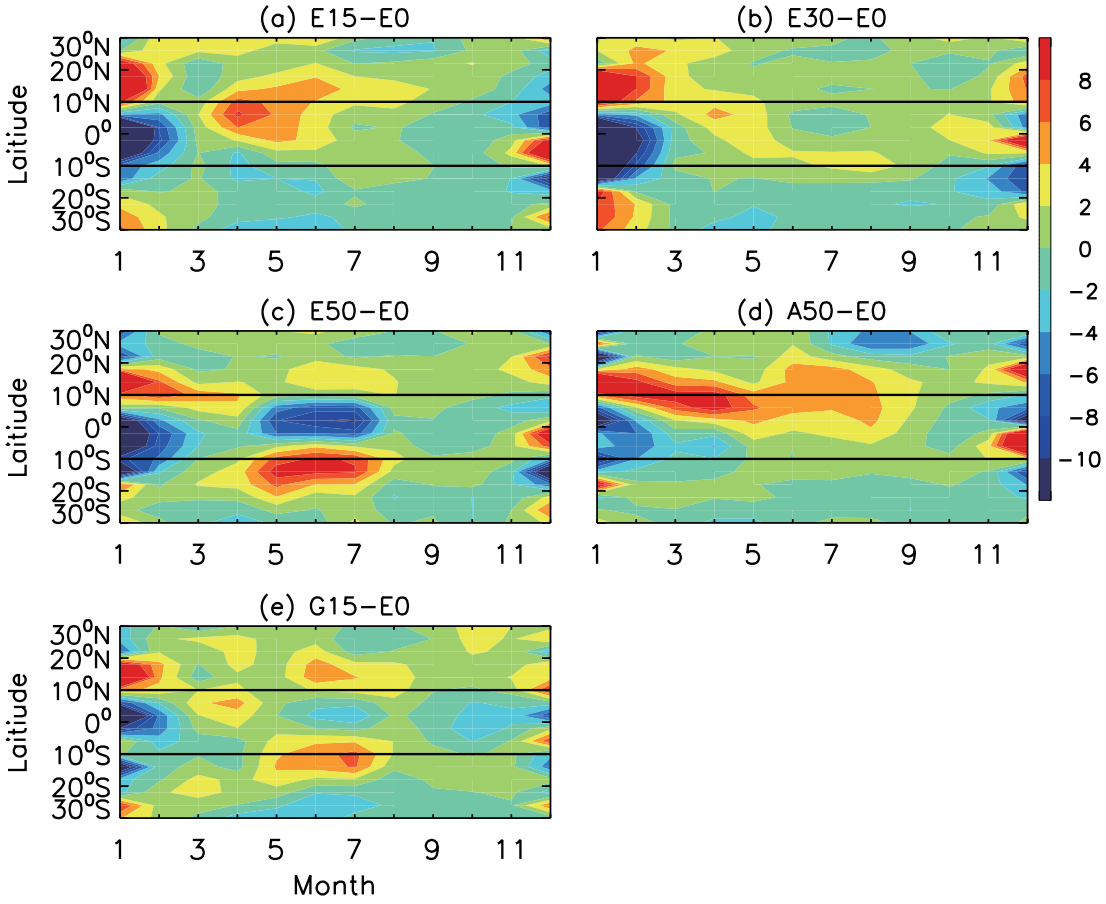

Fig. 4. Seasonal variation of BD circulation vertical velocity $\boldsymbol{w}^*$ ($-$Pa s^{-1}) at 100 hPa: the difference of (a) E15, (b) E30, (c) E50, (d) A50 and (e) G15, relative to E0.

indicated by the noteworthy vertical velocity increase in January and February and the slight increase in other months. Therefore, there is also a large increase of the total mass flux in G15 between 22°S and 30°N.

4. Effect of CH_4 emission increases on stratospheric and tropospheric ozone

Previous studies have shown that the tropospheric and stratospheric O_3 increases as CH_4 emissions increase (e.g., Owens et al., 1982, 1985; Isaksen and Stordal, 1986; Wuebbles and Hayhoe, 2002). Figure 5 shows the difference of stratospheric O_3 in E50, A50 and G15. In the middle stratosphere, CH_4 reacts with active chlorine ($CH_4 + Cl \rightarrow CH_3 + HCl$) and decreases catalytic O_3 loss caused by Cl radicals; this is the main cause of O_3 increase in the middle stratosphere.

When CH_4 emissions increase by 50% in East Asia (E50) and 15% on the global scale (G15), the maximum increase of stratospheric O_3 is 45 ppbv and 60 ppbv, respectively. Therefore, a CH_4 emissions increase is beneficial for stratospheric O_3 recovery. It should be noted that although the increment of CH_4 emissions in East Asia and North America is the same, the stratospheric O_3 increase in A50 is larger, and the maximum increase reaches 60 ppbv. That is to say, when CH_4 emissions increase by the same amount in East Asia and North America, the effect on the stratospheric O_3 of the former is less than the latter.

Around 90% of atmospheric CH_4 is removed through chemical reactions in the atmosphere, and 10% is removed by soil oxidation. Figure 6 shows the OH and O_3 difference in the troposphere between each sensitivity experiment and experiment E0. The reaction between CH_4 and OH radicals ($CH_4 + OH \rightarrow CH_3 + H_2O$) is the main removal mechanism of CH_4 in the troposphere. In the stratosphere, CH_4 reacts with the OH and $O^1(D)$ radical; however, the photolysis process of CH_4 can be ignored (e.g., Qin and Zhao, 2003). The photochemical reaction of the OH radical is important for oxidation and removal of numerous trace gases. In general, the concentration of the OH radical is highest in the tropics, and slightly higher in the Southern than the Northern Hemisphere [e.g., Chameides and Davis (1982)]. As shown in Figs. 6a and b, OH in the Northern Hemisphere significantly reduces as CH_4 oxidation by OH mainly occurs in the Northern Hemisphere when CH_4 emissions increase in East Asia and North America. CH_4 is oxidized by OH on the global scale in G15, so the tropospheric OH reduces uniformly in both hemispheres.

One quarter of the hydroxyl radicals react with CH_4, starting several oxidation chains that strongly affect the atmo-

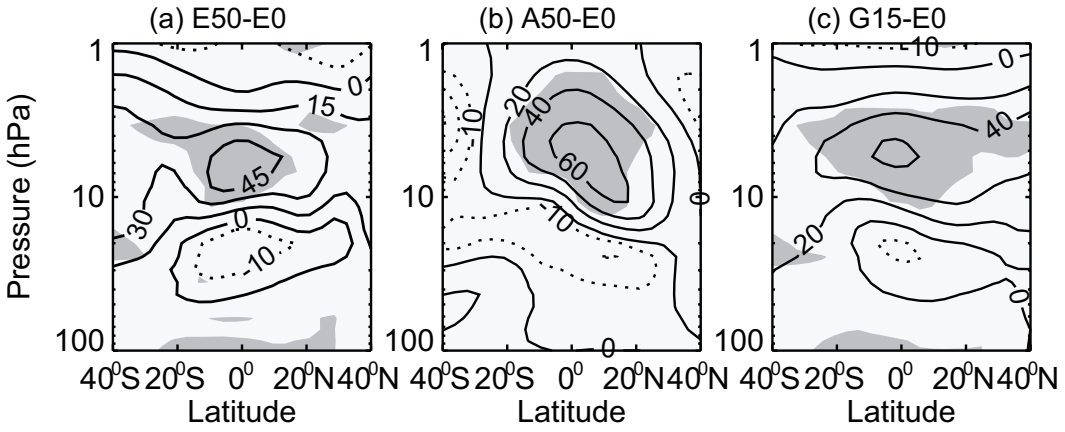

Fig. 5. Latitude–height cross sections of O_3 differences (units: ppbv) in (a) E50, (b) A50 and (c) G15, relative to E0. Shaded regions show where the differences are statistically significant at the 90% confidence level, using the Student's *t*-test.

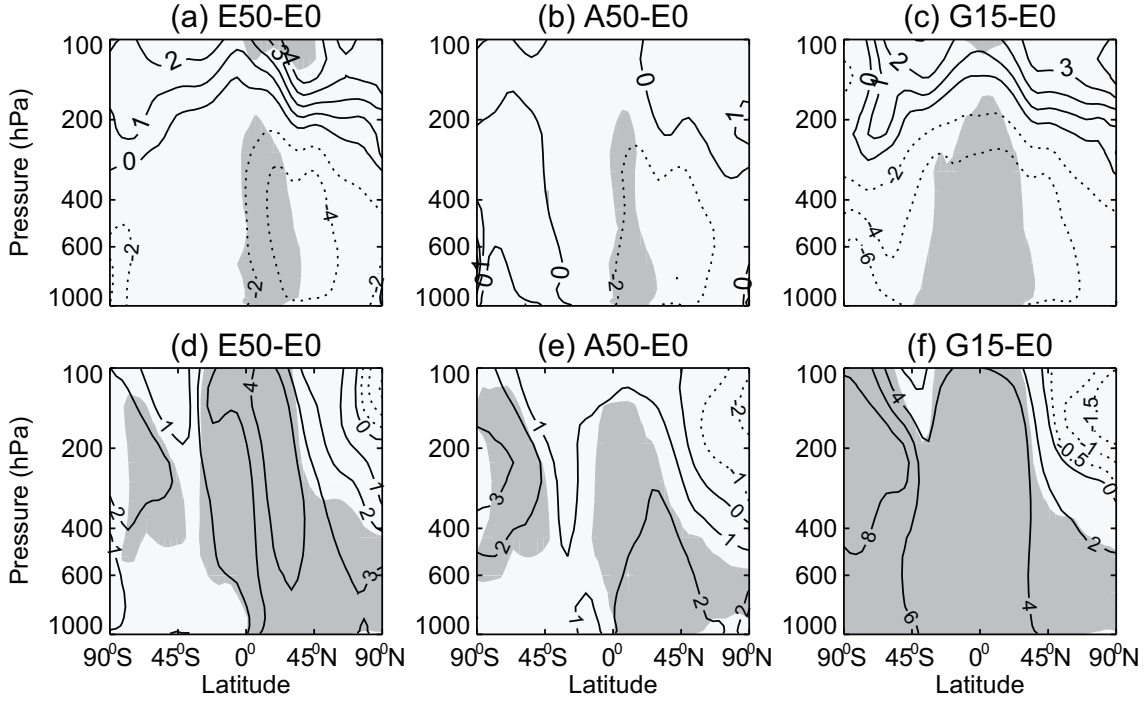

Fig. 6. Latitude–height cross sections (a–c) of OH differences (units: %) and (d–f) O_3 differences (units: %) of (a, d) E50, (b, e) A50 and (c, f) G15, compared with E0. Shaded regions show where the differences are statistically significant at the 90% confidence level, using the Student's *t*-test.

spheric concentrations of OH and O_3 (e.g., Crutzen, 1973). The availability of NO plays an important role in determining the oxidation pathways:

$$\mathrm{CH_4 + OH \rightarrow CH_3 + H_2O}$$
$$\mathrm{CH_3 + O_2 + M \rightarrow CH_3O_2 + M}$$
$$\mathrm{CH_3O_2 + NO \rightarrow CH_3O + NO_2}$$
$$\mathrm{CH_3O + O_2 \rightarrow CH_2O + HO_2}$$
$$\mathrm{HO_2 + NO \rightarrow OH + NO_2}$$
$$\mathrm{NO_2 + h\nu \rightarrow NO + O(\leqslant 400\ nm)}$$
$$\mathrm{O + O_2 + M \rightarrow O_3 + M}$$
$$\mathrm{Net: CH_4 + NO + 3O_2 \rightarrow CH_2O + H_2O + NO_2 + O_3}$$

CH_4 oxidation by OH mainly occurs in the Northern Hemisphere troposphere when CH_4 emissions increase in East Asia and North America. This causes O_3 to increase significantly in the Northern Hemisphere troposphere. The concentration of CH_4 is higher at high latitudes than at low latitudes. With the same percentage increase of CH_4 in East Asia and North America, the increment of CH_4 at high latitudes is larger than at low latitudes. But, as shown in Figs. 6d

and e, the maximum percentage increase of the tropospheric O_3 appears in the low-and midlatitudes. This is because CH_4 oxidation by OH mostly occurs in the tropics and the concentration of NO_x is largest in the midlatitudes (e.g., Fiore et al., 2008). It should be noted that OH reduces by 4%, and O_3 in the Northern Hemisphere midlatitudes increases by 4% in E50. There is a small variation in A50, with OH reducing by 2% and O_3 in the Northern Hemisphere midlatitudes increasing by 2%. It is also interesting that the altitude of the maximum changes of OH and O_3 is higher in E50 than in A50. This is because the concentration of OH is higher in East Asia than North America in the troposphere (not shown), and when CH_4 emissions increase in East Asia, CH_4 could be fully oxidized and generate more O_3 in the troposphere. When CH_4 emissions increase in North America, the oxidation reaction of CH_4 and OH is not sufficient, so more CH_4 is transported into the stratosphere, where it is oxidized, and more O_3 is generated in the stratosphere.

O_3 is generated through the CH_4 oxidation in the presence of NO_x in the troposphere (e.g., Crutzen, 1973). During the 20th century, global background O_3 concentrations rose by at least a factor of two, due mainly to increases in CH_4 and NO_x emissions (e.g., Marenco et al., 1994; Wang and Jacob, 1998). Therefore, the distribution of CH_4 and NO_x in the troposphere plays an important role in generating O_3 (e.g., Fiore et al., 2008).

Figure 7 shows O_3 differences at different heights. There is an obvious local impact of CH_4 emission increases, and the maximum increase of O_3 is 5% in E50 and 4% in A50 at 500 hPa. In the upper troposphere at 200 hPa, in E50 the O_3 concentration increases by 6% in East Asia, higher than surrounding regions. In A50 the O_3 concentration increment in North America is higher than surrounding regions, but the O_3 does not increase significantly in the other lower latitude regions, and the O_3 increment in North America is only 4%, much smaller than E50. The O_3 increase is symmetrically distributed along the equator in G15.

Tropospheric O_3 is an important greenhouses gas, and as a chemically active gas it can react with numerous active substances. High concentrations of tropospheric O_3 are harmful to health, affecting the respiratory system. When CH_4 emissions increase by the same amount in East Asia and North America, the effect on tropospheric O_3 in the former is larger than the latter.

Lang et al. (2012) found that the seasonal variation of O_3 change due to CH_4 emission increases in the troposphere is very weak, except near the tropical tropopause where O_3 has a maximum increase in July. As shown in Fig. 7, the local change of tropospheric O_3 is significant when CH_4 emissions increase in East Asia and North America; therefore, the O_3 changes in different months in East Asia and North America are interesting. The distribution of tropospheric O_3 concentrations in East Asia and North America are shown in Fig. 8a, and are in good agreement with Wang et al. (2006). As shown in Fig. 8b, there is an obvious seasonal variation of O_3 change in East Asia when CH_4 emissions increase in East Asia in the upper troposphere (200 hPa). The maximum increment appears in August. The seasonal variation of O_3 change in

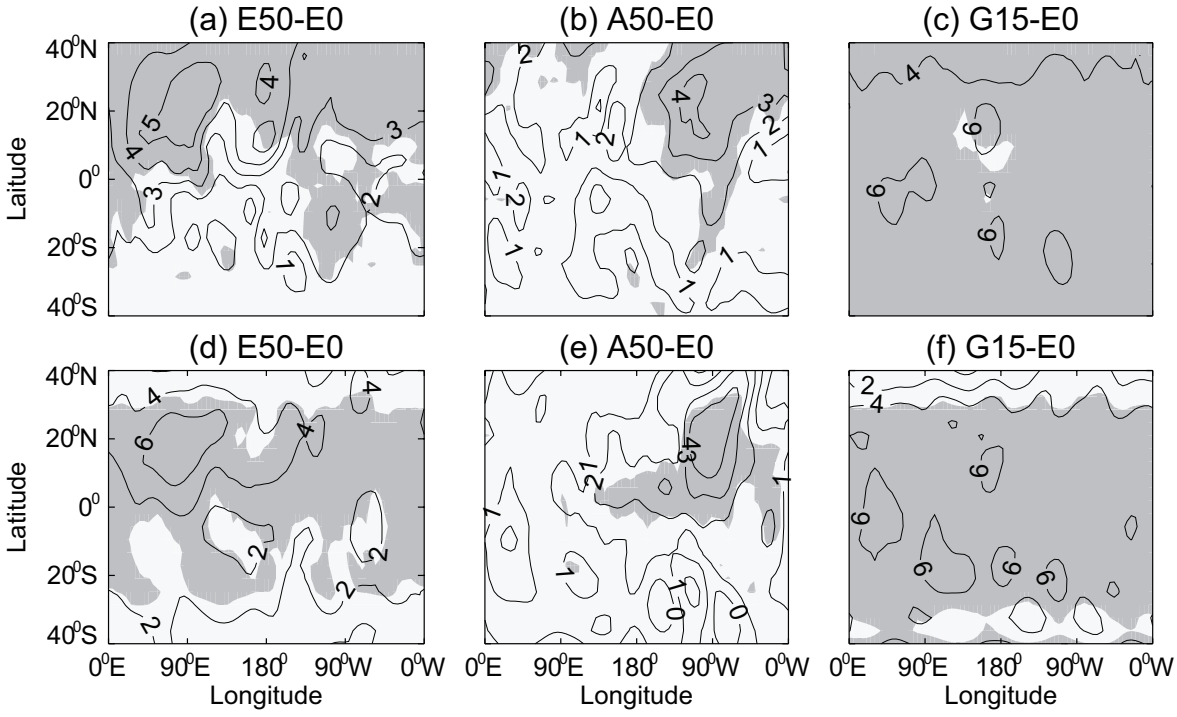

Fig. 7. Longitude–latitude cross sections of O_3 differences (units: %) at (a–c) 500 hPa and (d–f) 200 hPa in (a, d) E50, (b, e) A50 and (c, f) G15, compared with E0. Shaded regions show where the differences are statistically significant at the 90% confidence level, using the Student's *t*-test.

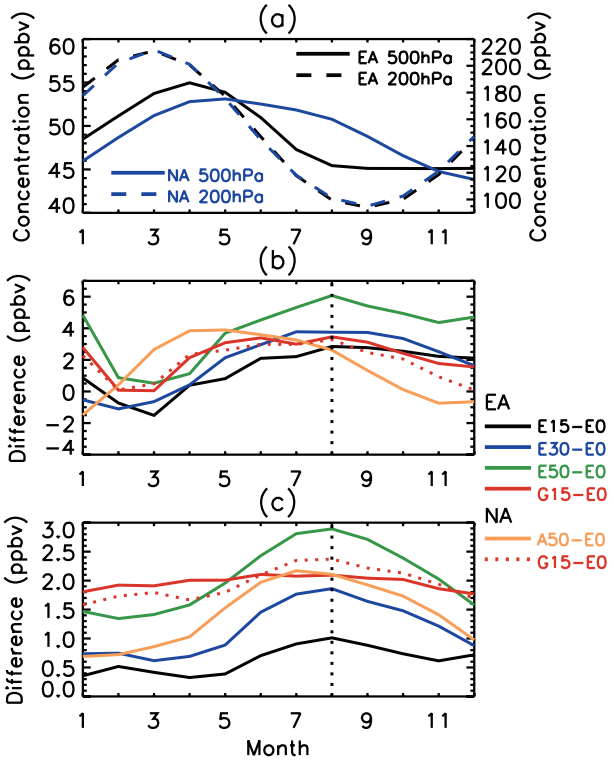

Fig. 8. (a) Annual average O_3 for different months simulated by the control experiment (E0) in East Asia (black) and North America (blue). Dotted and solid lines indicate simulations at 200 hPa (left vertical axis) and 500 hPa (right vertical axis). (b) Differences of annual average O_3 during different months of the sensitivity experiments compared with E0 at 200 hPa. (c) As in (b) but for 500 hPa. The results for E15 (black), E30 (blue), E50 (green), and G15 (red solid line) indicate the difference compared with E0 in East Asia. The results for A50 (orange) and G15 (red dotted line) indicate the difference compared with E0 in North America.

North America in A50 shows that the maximum increment appears in April. In G15, the variation is small in different months and the increment of O_3 is large from May to September.

O_3 increases are more consistent at 500 hPa than at 200 hPa, as the maximum increment of O_3 concentration appears in August in East Asia and in July in North America. However, the seasonal variation of O_3 change in G15 is not obvious (Fig. 8c) in either East Asia or North America. This proves that seasonal variation of O_3 concentrations, shown in Fig. 8, are affected by CH_4 emission increases locally in the lower troposphere. Comparing Figs. 8a–c, the maximum O_3 increment appears when the original O_3 concentration is at its minimum in East Asia, so the percentage change of O_3 concentration is similar to Figs. 8b and c. Although the O_3 concentration increase is smaller in the middle troposphere than in the upper troposphere, the seasonal variation is also significant in the middle troposphere. The O_3 concentration is lower at 500 hPa than 200 hPa, so the percentage change of O_3 concentration is larger at 500 hPa than 200 hPa (not shown).

Since CH_4 oxidation by OH depends on temperature, when CH_4 emissions increase the largest O_3 concentration increment should be in summer. But in A50, the maximum increment appears in April at 200 hPa. The seasonal variation of O_3 change in A50 is inconsistent with the seasonal variation of O_3 concentration simulated by the control experiment shown in Figs. 8a and b. That is, the O_3 concentration change in A50 at 200 hPa is caused by transport processes. So, when CH_4 emissions increase in East Asia, its impact on the tropospheric O_3 can be noted throughout the troposphere. However, when CH_4 emissions increase in North America, the impact on the tropospheric O_3 can be noted only in the lower troposphere and the change of O_3 concentration in the upper troposphere is caused by transport processes.

5. Summary and conclusions

A fully coupled chemistry–climate model (WACCM3) was used to investigate the effect of CH_4 emission increases, especially in East Asia and North America, on atmospheric temperature, circulation and O_3.

The results show that CH_4 emission increases can strengthen the westerly winds in the Northern Hemisphere midlatitudes, and accelerate the BD circulation, increasing the mass flux across the tropopause. However, the tropical BD circulation between 10°S and 10°N at 100 hPa becomes weaker when CH_4 emissions increase in East Asia, and stronger when CH_4 emissions increase in North America. When CH_4 emissions increase by 50% in East Asia and 15% globally, the stratospheric temperature cools by up to 0.15 K, and the stratospheric O_3 increases by 45 ppbv and 60 ppbv, respectively. When CH_4 emissions increase by 50% in North America the stratospheric O_3 increases by 60 ppbv, so it has a greater influence on stratospheric O_3 than the effect of a CH_4 emissions increase of the same amount in East Asia. CH_4 increases in East Asia and North America can reduce the tropospheric OH concentration (4% and 2%, respectively) and increase the tropospheric O_3 concentration (5% and 4%, respectively) in the Northern Hemisphere midlatitudes. When CH_4 increases in East Asia, the increase of the tropospheric O_3 concentration is largest in August. When CH_4 increases in North America, the increase of the O_3 concentration reaches a maximum in July in the middle troposphere, and in April in the upper troposphere. When CH_4 emissions increase in East Asia, the impact on tropospheric O_3 can be noted throughout the troposphere. However, when CH_4 emissions increase in North America, the impact on tropospheric O_3 is notable only in the lower troposphere and the change of O_3 concentration in the upper troposphere is caused by transport processes.

The emissions scenarios used in this paper are provided by the IPCC at a resolution of $4^\circ \times 5^\circ$, so the CH_4 emissions source is coarse. CH_4 reacts with CO, NO_x and other chemical substances, affecting tropospheric O_3 and stratospheric climate. Against the background of increasing pollutant emissions, the effect of a CH_4 emissions increase must be associated with CO, NO_x and other substances. There-

fore, much more work is needed to fully understand the effect of CH_4 emission increases on both tropospheric and stratospheric climate in East Asia.

Acknowledgements. This work was supported by the China High Resolution Earth Observation Project (Grant No. 1-113406) and the National Science Foundation of China (Grant Nos. 41225018 and 41175042).

REFERENCES

Andrews, D. G., and M. E. McIntyre, 1976: Planetary waves in horizontal vertical shear: The generalized Eliassen–Palm relation and the mean zonal acceleration. *J. Atmos. Sci.*, **33**, 2031–2048.

Andrews, D. G., and M. E. McIntyre, 1978: Generalized Eliassen–Palm and Charney–Drazin theorems for waves on axismmetric mean flows in compressible atmospheres. *J. Atmos. Sci.*, **35**, 175–185.

Austin, J., and F. Li, 2006: On the relationship between the strength of the Brewer-Dobson circulation and the age of stratospheric air. *Geophys. Res. Lett.*, **33**, L17807, doi: 10.1029/2006GL026867.

Austin, J., J. Wilson, F. Li, and H. Vömel, 2007: Evolution of water vapor concentrations and stratospheric age of air in coupled chemistry-climate model simulations. *J. Atmos. Sci.*, **64**(3), 905–921.

Bergamaschi, P., and Coauthors, 2013: Atmospheric CH_4 in the first decade of the 21st century: Inverse modeling analysis using SCIAMACHY satellite retrievals and NOAA surface measurements. *J. Geophys. Res.*, **118**(13), 7350–7369.

Bi, Y., 2009: Study on the distributions, variations and climate impacts of the water vapor and methane in stratosphere. Ph.D. dissertation, Space Physics, University of Science and Technology of China, 149 pp. (in Chinese)

Bi, Y., Y. J. Chen, L. Xu, S. M. Deng, and R. J. Zhou, 2007: Analysis of H_2O and CH_4 distribution characteristics in the middle atmosphere using HALOE data. *Chinese Journal of Atmospheric Sciences*, **31**(3), 440–448. (in Chinese with English abstract)

Bi, Y., Y. J. Chen, R. J. Zhou, M. H. Fang, and L. Xu, 2008: Study on H_2O and CH_4 distributions and variations over Qinghai-Xizang Plateau using HALOE data. *Plateau Meteorology*, **27**(2), 249–258. (in Chinese with English abstract)

Born, M., H. Dörr, and I. Levin, 1990: Methane consumption in aerated soils of the temperate zone. *Tellus B*, **42**(1), 2–8.

Brasseur, G. P., D. A. Hauglustaine, S. Walters, P. J. Rasch, J. -F. Müller, C. Granier, and X. X. Tie, 1998: MOZART: A global chemical transport model for ozone and related chemical tracers: 1. Model description. *J. Geophys. Res.*, **103**, 28 265–28 289.

Butchart, N., and A. A. Scaife, 2001: Removal of chlorofluorocarbons by increased mass exchange between the stratosphere and troposphere in a changing climate. *Nature*, **410**(6830), 799–802.

Butchart, N., and Coauthors, 2006: Simulations of anthropogenic change in the strength of the Brewer-Dobson circulation. *Climate Dyn.*, **27**(7–8), 727–741.

Chameides, W. L., and D. D. Davis, 1982: The free radical chemistry of cloud droplets and its impact upon the composition of rain. *J. Geophys. Res.*, **87**(C7), 4863–4877.

Chappellaz, J., J. M. Barnola, D. Raynaud, Y. S. Korotkevich, and C. Lorius, 1990: Ice-core record of atmospheric methane over the past 160, 000 years. *Nature*, **345**(6271), 127–131.

Chen, Y. J., R. J. Zhou, C. H. Shi, and Y. Bi, 2006: Study on the trace species in the stratosphere and their impact on climate. *Adv. Atmos. Sci.*, **23**(6), 1020–1039, doi: 10.1007/s00376-006-1020-3.

Collins, W. D., and Coauthors, 2004: Description of the NCAR Community Atmosphere Model (CAM3). Tech. Note NCAR/TN-464+STR, Natl. Center for Atmos. Res., 226 pp.

Crutzen, P., 1973: A discussion of the chemistry of some minor constituents in the stratosphere and troposphere. *Pure Appl. Geophys.*, **106**(1), 1385–1399.

Dyominov, I. G., and A. M. Zadorozhny, 2005: Greenhouse gases and recovery of the Earth's ozone layer. *Advances in Space Research*, **35**, 1369–1374.

Eichelberger, S. J., and D. L. Hartmann, 2005: Changes in the strength of the Brewer-Dobson circulation in a simple AGCM. *Geophys. Res. Lett.*, **32**, L15807, doi: 10.1029/2005GL022924.

Eyring, V., and Coauthors, 2010: Multi-model assessment of stratospheric ozone return dates and ozone recovery in CCMVal-2 models. *Atmospheric Chemistry and Physics*, **10**(19), 9451–9472.

Fiore, A. M., J. J. West, L. W. Horowitz, V. Nail, and M. D. Schwarzkopf, 2008: Characterizing the tropospheric ozone response to methane emission controls and the benefits to climate and air quality. *J. Geophys. Res.*, **113**, D08307, doi: 10.1029/2007JD009162.

Fomichev, V. I., A. I. Jonsson, J. de Grandpre, S. R. Beagley, C. McLandress, K. Semeniuk, and T. G. Shepherd, 2007: Response of the middle atmosphere to CO_2 doubling: Results from the Canadian Middle Atmosphere Model. *J. Climate*, **20**(7), 1121–1144.

Fuglestvedt, J. S., I. S. A. Isaksen, and W. C. Wang, 1996: Estimates of indirect global warming potentials for CH_4, CO and NO_x. *Climatic Change*, **34**(3–4), 405–437.

Garcia, R. R., and W. J. Randel, 2008: Acceleration of the Brewer-Dobson circulation due to increases in greenhouse gases. *J. Atmos. Sci.*, **65**, 2731–2739.

Garcia, R. R., D. R. Marsh, D. E. Kinnison, B. A. Boville, and F. Sassi, 2007: Simulation of secular trends in the middle atmosphere, 1950–2003. *J. Geophys. Res.*, **112**, D09301, doi: 10.1029/2006JD007485.

Garny, H., M. Dameris, W. Randel, G. E. Bodeker, and R. Deckert, 2011: Dynamically forced increase of tropical upwelling in the lower stratosphere. *J. Atmos. Sci.*, **68**, 1214–1233.

Gruzdev, A. N., and G. P. Brasseur, 2005: Long-term changes in the mesosphere calculated by a two-dimensional model. *J. Geophys. Res.*, **110**, 304–321.

Guo, S. C., H. Zhou, D. R. Lv, Y. Q. Li, M. Dai, and Q. Li, 2008: Temporal and spatial features of atmospheric methane and its relation to ozone variation in the stratosphere. *Journal of Yunnan University (Natural Sciences Edition)*, **30**(4), 381–387. (in Chinese with English abstract)

Hall, T. M., and R. A. Plumb, 1994: Age as a diagnostic of stratospheric transport. *J. Geophys. Res.*, **99**(D1), 1059–1070.

Hauglustaine, D. A., G. P. Brasseur, S. Walters, P. J. Rasch, J. -F. Müller, L. K. Emmons, and M. A. Carroll, 1998: MOZART: A global chemical transport model for ozone and related chemical tracers: 2. Model results and evaluation. *J. Geophys. Res.*, **103**, 28 291–28 335.

Holton, J. R., 1990: On the global exchange of mass between the stratosphere and troposphere. *J. Atmos. Sci.*, **48**, 392–395.

Horowitz, L. W., and Coauthors, 2003: A global simulation of tropospheric ozone and related tracers: Description and evaluation of MOZART, version 2. *J. Geophys. Res.*, **108**(D24), doi: 10.1029/2002JD002853.

IPCC, 2007: *Climate Change 2007: The Physical Science Basis. Contribution of Working Group I to the Fourth Assessment Report of the Intergovernmental Panel on Climate Change*. Cambridge University Press, New York, 996 pp.

Isaksen, I. S. A., and F. Stordal, 1986: Antarctic ozone depletion: 2-D model studies. *Geophys. Res. Lett.*, **13**(12), 1327–1330.

Lang, C., and Coauthors, 2012: The impact of greenhouse gases on past changes in tropospheric ozone. *J. Geophys. Res.*, **117**, D23304, doi: 10.1029/2012JD018293.

Lelieveld, J., and P. J. Crutzen, 1992: Indirect chemical effects of methane on climate warming. *Nature*, **355**, 339–342.

Lelieveld, J., P. J. Crutzen, and F. J. Dentener, 1998: Changing concentration, lifetime and climate forcing of atmospheric methane. *Tellus B*, **50**(2), 128–150.

Levy, H. II., 1971: Normal atmosphere: Large radical and formaldehyde concentrations predicted. *Science*, **173**, 141–143.

Lin, P., and Q. Fu, 2013: Changes in various branches of the Brewer-Dobson circulation from an ensemble of chemistry climate models. *J. Geophys. Res.*, **118**(1), 73–84.

Liu, Y., and C. X. Liu, 2009: Simulation studies on seasonal variations of the stratospheric dynamics and trace gases using coupled chemistry-climate model WACCM-3. *Chinese Journal of Space Science*, **29**(6), 580–590. (in Chinese with English abstract)

Marenco, A., H. Gouget, P. Nédélec, J. -P. Pagés, and F. Karcher, 1994: Evidence of a long-term increase in tropospheric ozone from Pic du Midi data series: Consequences: Positive radiative forcing. *J. Geophys. Res.*, **99**(D8), 16 617–16 632.

Olsen, M. A., M. R. Schoeberl, and J. E. Nielsen, 2007: Response of stratospheric circulation and stratosphere-troposphere exchange to changing sea surface temperatures. *J. Geophys. Res.*, **112**, D16104, doi: 10.1029/2006JD008012.

Owens, A. J., J. M. Steed, D. L. Filkin, C. Miller, and J. P. Jesson, 1982: The potential effects of increased methane on atmospheric ozone. *Geophys. Res. Lett.*, **9**(9), 1105–1108.

Owens, A. J., C. H. Hales, D. L. Filkin, C. Miller, J. M. Steed, and J. P. Jesson, 1985: A coupled one-dimensional radiative-convective, chemistry-transport model of the atmosphere: 1. Model structure and steady state perturbation calculations. *J. Geophys. Res.*, **90**, 2283–2311.

Qin, Y., and C. S. Zhao, 2003: *Basic Atmospheric Chemistry*. Meteorology Press, 202 pp. (in Chinese)

Ramaswamy, V., and Coauthors, 2001: Radiative forcing of climate change. *Climate Change 2001: The Scientific Basis*, J. T. Houghton et al., Eds., Cambridge University Press, New York, 349–416.

Rasmussen, R. A., and M. A. K. Khalil, 1984: Atmospheric methane in the recent and ancient atmospheres: Concentrations, trends, and interhemispheric gradient. *J. Geophys. Res.*, **89**(D7), 11 599–11 605.

Rayner, N. A., and Coauthors, 2003: Global analyses of sea surface temperature, sea ice, and night marine air temperature since the late nineteenth century. *J. Geophys. Res.*, **108**(D14), doi: 10.1029/2002JD002670.

Rind, D., J. Lerner, and C. McLinden, 2001: Changes of tracer distributions in the doubled CO_2 climate. *J. Geophys. Res.*, **106**(D22), 28 061–28 079.

Shi, C. H., 2006: Study on the trends and chemical process of trace gases in stratosphere. PhD. dissertation, Space Physics, University of Science and Technology of China, 191 pp. (in Chinese)

Shi, C. H., B. Zheng, Y. J. Chen, and Y. Bi, 2009: The quasi-biennial oscillation of water vapor in tropical stratosphere. *Chinese Journal of Geophysics*, **52**(10), 2428–2435. (in Chinese with English abstract)

Shindell, D. T., G. Faluvegi, N. Bell, and G. A. Schmidt, 2005: An emissions-based view of climate forcing by methane and tropospheric ozone. *Geophys. Res. Lett.*, **32**(4), L04803, doi: 10.1029/2004GL021900.

Sigmond, M., P. C. Siegmund, E. Manzini, and H. Kelder, 2004: A simulation of the separate climate effects of middle-atmospheric and tropospheric CO_2 doubling. *J. Climate*, **17**(12), 2352–2367.

Stevenson, D., and Coauthors, 2006: Multimodel ensemble simulations of present-day and near-future tropospheric ozone. *J. Geophys. Res.*, **111**(D8), doi: 10.1029/2005JD006338.

Wang, Y. H., and D. J. Jacob, 1998: Anthropogenic forcing on tropospheric ozone and OH since preindustrial times. *J. Geophys. Res.*, **103**(D23), 31 123–31 135.

Wang, W. G., M. Yuan, J. Wu, W. X. Fan, H. Y. Wang, and X. L. Liu, 2006: The variation of spatial temporal distribution of the global tropopause ozone. *Journal of Yunnan University (Natural Sciences Edition)*, **28**(6), 509–517. (in Chinese with English abstract)

Waugh, D., and T. Hall, 2002: Age of stratospheric air: Theory, observations, and models. *Rev. Geophys.*, **40**, 1-1–1-26.

Wild, O., and P. I. Palmer, 2008: How sensitive is tropospheric oxidation to anthropogenic emissions? *Geophys. Res. Lett.*, **35**(22), doi: 10.1029/2008GL035718.

Wuebbles, D. J., and K. Hayhoe, 2002: Atmospheric methane and global change. *Earth-Science Reviews*, **57**(3–4), 177–210.

Xie, F., W. S. Tian, J. P. Li, J. K. Zhang, and L. Shang, 2013: The possible effects of future increase in methane emission on the stratospheric water vapor and global ozone. *Acta Meteorologica Sinica*, **71**(3), 555–567. (in Chinese with English abstract)

Zhang, R. J., M. X. Wang, and Y. S. Wang, 2001: Long-term trends of atmospheric methane and its future change. *Climate and Environmental Research*, **6**(1), 53–57. (in Chinese with English abstract)

Zhang, X. Y., W. G. Bai, P. Zhang, and W. H. Wang, 2011: Spatiotemporal variations in mid-upper tropospheric methane over China from satellite observations. *Chinese Science Bulletin*, **56**, 3321–3327.